*Inorg. Chem.* **2008**, *47*, 9097−9102

Inorganic Chemistry
Article

# Hydrothermal Synthesis of Vanadium Oxyfluoride Chains Incorporating Covalently Bound Copper Coordination Complexes

**Thushitha Mahenthirarajah, Yang Li, and Philip Lightfoot***

*EaStChem, School of Chemistry, University of St. Andrews, St. Andrews, Fife, KY16 9ST, United Kingdom*

Received June 16, 2008

An exploration of the hydrothermal synthesis of vanadium oxyfluorides in the presence of copper−amine coordination complexes has produced six new compounds exhibiting novel one-dimensional structural features. $[C_2H_8N][Cu(C_5H_5N)_4][V_2O_2F_7]$ incorporates dimeric vanadium(IV) oxyfluoride units (in this case, face-sharing V-centered octahedra) into a compound of this type for the first time; this composition has been prepared in two polymorphs, **1** and **2**, which differ in chain configuration and orientation, mediated by H bonding of the uncoordinated dimethylammonium cation. A differing dimeric vanadium(IV) oxyfluoride anion (based on edge-sharing V-centered octahedra) occurs in $[C_3H_5N_2]_2[Cu(C_3H_4N_2)_4][V_2O_2F_8]$, **4**, which incorporates imidazole in two structural roles: as both a ligand and template. $[Cu_2F_2(C_{10}H_{10}N_3)_2][V_2O_7]$, **5**, and $[Cu(C_5H_5N)_2(C_2H_8N_2)][(VO_3)_2]$, **6**, both contain $V^{5+}$ in tetrahedral coordination, in dimers in the former and infinite chains in the latter. In the case of **6**, the copper moieties act as "decoration" rather than as linkers to the vanadium oxide sublattice.

## Introduction

Vanadium has a rich and complex aqueous chemistry, and vanadium oxide based chemistry becomes even more rich and complex on entering the solid state. Considerable effort has been aimed at defining the vanadium-containing "building blocks" present in vanadium oxide chemistry and the structural systematics of vanadium oxides in general[1] and, more specifically, those obtained from solvothermal reactions, including organic "structure-directing agents" (SDAs).[2,3] Extending this work beyond oxides, there has been much work on phosphates, phosphonates, carboxylates, and other oxyanion derivatives;[4−6] many of these hybrid materials are prepared in fluoride-containing media (usually merely to aid crystallization) and often contain fluoride in addition to the oxyanion species. Although there have been recent attempts specifically to understand the nature of fluoride incorporation into these compounds, the inherent complexity of such systems[7] currently negates the possibility of a clear understanding of the experimental factors leading to particular structural features. We have recently initiated a more focused study of vanadium oxyfluoride (VOF) solvothermal and structural chemistry, targeting systems which contain typical organic SDAs but which do not contain anionic ligands in addition to fluoride. We have found a variety of oligomeric VOF units[8,9] which, depending on reaction conditions, may condense into chain, ladder, or layer structures.[10−12] However, although we have achieved some success in preparing optically and magnetically active materials, the control and prediction of particular structural features in these compounds, especially those "extended" features which might lead to functionality, are ultimately lacking.

* Author to whom correspondence should be addressed. E-mail: pl@st-and.ac.uk.

(1) Zavalij, P. Y.; Whittingham, M. S. *Acta Crystallogr.* **1999**, *B55*, 627.
(2) Hagrman, P. J.; Finn, R. C.; Zubieta, J. *Solid State Sci.* **2001**, *3*, 745.
(3) Chirayil, T.; Zavalij, P. Y.; Whittingham, M. S. *Chem. Mater.* **1998**, *10*, 2629.
(4) Finn, R. C.; Zubieta, J.; Haushalter, R. C. *Prog. Inorg. Chem.* **2003**, *51*, 421.
(5) Ouelette, W.; Yu, M.-H.; O'Connor, C. J.; Zubieta, J. *Inorg. Chem.* **2006**, *45*, 3224.
(6) Barthelet, K.; Adil, K.; Millange, F.; Serre, C.; Riou, D.; Férey, G. *J. Mater. Chem.* **2003**, *13*, 2208.
(7) Ouelette, W.; Golub, V.; O'Connor, C. J.; Zubieta, J. *Dalton Trans.* **2005**, 291.
(8) Stephens, N. F.; Buck, M.; Lightfoot, P. *J. Mater. Chem.* **2005**, *15*, 4298.
(9) Aldous, D. W.; Stephens, N. F.; Lightfoot, P. *Dalton Trans.* **2007**, 2271.
(10) Aldous, D. W.; Stephens, N. F.; Lightfoot, P. *Inorg. Chem.* **2007**, *46*, 4207.
(11) Aldous, D. W.; Goff, R. J.; Attfield, J. P.; Lightfoot, P. *Inorg. Chem.* **2007**, *46*, 1277.
(12) Aldous, D. W.; Stephens, N. F.; Lightfoot, P. *Inorg. Chem.* **2007**, *46*, 3996.

10.1021/ic801106h CCC: $40.75 
Published on Web 08/19/2008

In order to introduce a "design" element to direct and control the interactions between anionic VOF units and related species in the solid state, Poeppelmeier and co-workers have devised strategies which employ, for example, cationic copper coordination complexes as linkers.[13,14] This approach has proved successful in preparing and rationalizing the formation of chiral and polar crystals in such systems. So far, the Cu−VOFs reported by Poeppelmeier have contained solely $[Cu(py)_4]^{2+}$ as the linker and the monomeric anionic units $[VOF_5]^{2-}$ and $[VOF_4]^{2-}$. Very recently, we described the synthesis and crystal structure of the first fully three-dimensional example of a VOF linked by $[Cu(py)_4]^{2+}$ units.[15] In this work, we seek to expand on these studies, by employing a wider variety of copper-containing species, which in turn leads to the isolation of compounds containing novel structural features, for example, chain structures containing dimeric rather than monomeric VOF units.

## Experimental Section

**Synthesis.** α-$[C_2H_8N][Cu(C_5H_5N)_4][V_2O_2F_7]$, **1**; β-$[C_2H_8N][Cu(C_5H_5N)_4][V_2O_2F_7]$, **2**; $[Cu(C_6H_7N)_4][VF_6]$, **3**; $[C_3H_5N_2]_2[Cu(C_3H_4N_2)_4][V_2O_2F_8]$, **4**; $[Cu_2F_2(C_{10}H_{10}N_3)_2][V_2O_7]$, **5**; and $[Cu(C_5H_5N)_2(C_2H_8N_2)][(VO_3)_2]$, **6**, were all synthesized hydrothermally, in 27 mL Teflon-lined stainless steel autoclaves heated at 160 °C. A general scheme for synthesis is as follows. For single crystals of **1**, initially 0.200 g ($1.09 \times 10^{-3}$mol) of $V_2O_5$ was weighed into a 27 mL Teflon-lined stainless steel autoclave and dissolved with 0.5 mL ($2.89 \times 10^{-2}$ mol) of 48% HF at room temperature for 5 min. To the resultant solution were added 5 mL ($6.18 \times 10^{-2}$ mol) of pyridine, 0.15 g ($2.26 \times 10^{-3}$ mol) of trimethylamine-N-oxide, 0.5 mL ($2.77 \times 10^{-2}$ mol) of water, and finally 0.1 g ($1.25 \times 10^{-3}$mol) of CuO, and these were stirred well until fully dissolved. The preparation of single crystals of **2** follows the same reaction conditions as for **1**, but dimethylamine, 0.5 mL ($1.10 \times 10^{-2}$ mol), was used instead of trimethylamine-N-oxide. For single crystals of **3**, all reactant ratios are the same as for **1**, but 3-methylpyridine only was used as the amine source instead of pyridine and trimethylamine-N-oxide. A similar procedure was followed for **4**, but the reactants and ratios are different: 0.100 g ($0.54 \times 10^{-3}$ mol) of $V_2O_5$, 0.1 g ($1.25 \times 10^{-3}$ mol) of CuO, 0.3 mL ($1.73 \times 10^{-2}$ mol) of 48% HF, 0.3 mL ($1.662 \times 10^{-2}$ mol) of water, 10 mL ($12.36 \times 10^{-2}$ mol) of 3-methylpyridine, and 0.200 g ($2.93 \times 10^{-2}$ mol) of imidazole. For the preparation of single crystals of **5**, the reactants and ratios are 0.100 g ($0.54 \times 10^{-3}$ mol) of $V_2O_5$, 0.05 g ($0.62 \times 10^{-3}$ mol) of CuO, 0.2 mL ($1.15 \times 10^{-2}$ mol) of 48% HF, 10 mL ($5.54 \times 10^{-1}$ mol) of water, and 0.2 g ($1.16 \times 10^{-2}$ mol) of 2,2′-dipyridylamine. Single crystals of **6** were synthesized according to the following reactant ratios: 0.200 g ($1.09 \times 10^{-3}$ mol) of $V_2O_5$, 0.1 g ($1.25 \times 10^{-3}$ mol) of CuO, 0.5 mL ($2.89 \times 10^{-2}$ mol) of 48% HF, 0.5 mL ($2.77 \times 10^{-2}$ mol) of water, 10 mL ($1.23 \times 10^{-1}$ mol) of pyridine, and 0.2 mL ($3.3 \times 10^{-2}$ mol) of ethylenediamine. In each case, the reaction vessel was sealed and heated to 160 °C for 24 h and then cooled to room temperature over an additional 24 h. Crystals were recovered by vacuum filtration. Phase purity was ascertained by elemental analysis (CHN), together with a comparison of observed and simulated powder X-ray diffraction patterns. Elemental and crystallographic analyses are in reasonable agreement with the structural formula.

Complex **1**. Anal. calcd: C, 38.09%; H, 4.04%; N, 10.10%. Found: C, 37.59%; H, 3.77%; N, 9.57%, revealing that the template had broken down *in situ*.

Complex **2**. Anal. calcd: C, 38.09%; H, 4.04%; N, 10.10%. Found: C, 37.50%; H, 4.49%; N, 9.98%.

Complex **3**. Anal. calcd: C, 48.2%; H, 4.05%; N, 9.38%. Found: C, 47.70%; H, 4.41%; N, 9.38%.

Compex **5**. Anal. calcd: C, 33.02%; H, 2.49%; N, 11.55%. Found: C, 32.94%; H, 2.28%; N, 11.25%. In the cases of **4** and **6**, the major product was found to be mixed with uncharacterized phases. It should also be noted that **1**, **2**, **4**, and **6** are unstable in the air at room temperature, losing crystallinity within a few hours.

**Crystallography.** Single-crystal X-ray diffraction data were collected with on a Rigaku Mercury CCD with silicon monochromated graphite monochromated Mo Kα radiation. All of the data sets were corrected for absorption via multiscan methods. The structures were solved by direct methods and refined by full-matrix least-squares techniques, using the SHELXS, SHELXL, and WinGX packages. The final refinement includes anisotropic refinement for all non-hydrogen atoms, except the fluorine atoms in **3**, which were refined isotropically, due to disorder. Hydrogen atoms were fixed and refined using a riding model with isotropic displacement parameters. Crystallographic details are given in Table 1. In **2**, there is some evidence from the refinement of the incorporation of additional guest moieties, though these could not be conclusively assigned as either guest dimethylamine or water, either from the X-ray data or analytical data.

**Magnetic Measurements.** Magnetic susceptibility data for **1** and **3** were measured on a Quantum Design MPMS SQUID. Data were recorded in a 5000 Oe field while warming the sample from 2 to 300 K in 4 K steps, following consecutive zero-field cooling and field cooling cycles. The data were normalized to the molar quantity of the sample, and any diamagnetic contributions were deducted from the total magnetic contribution before data fitting.

## Results and Discussion

**Crystal Structures.** There are currently only four structures reported in the Cambridge Database having −V−F−Cu− connectivity.[7,13,14] Five out of six of the present cases exhibit a novel structural motif in vanadium oxyfluoride chemistry.

The crystal structure of **1** contains an infinite 1-D chain motif running parallel to the *c* axis, which is constructed by face-sharing octahedral dimers, $[V_2O_2F_7]^{3-}$, covalently bound through F to $[Cu(py)_4]^{2+}$ cations in an alternating manner. This basic building unit is shown in Figure 1, with the unit cell packing in Figure 2. The $Cu^{2+}$ center exhibits a characteristic Jahn−Teller environment, with four short Cu−N bonds and two long, axial Cu−F bonds, and the $V^{4+}$ exhibits a characteristically short V═O and lengthened trans V−F bond (Table 2). The $[V_2O_2F_7]^{3-}$ anion is the same as that previously reported in $Cs_3V_2O_2F_7$ by Pausewang,[16] and structurally charactreized by Waltersson,[17] though in that case the anion exhibited crystallographic disorder of the terminal O/F positions. The dimethylammonium cations are accommodated in the interchain region, forming hydrogen bonds

(13) Welk, M. E.; Stern, C. L.; Poeppelmeier, K. R.; Norquist, A. J. *Cryst. Growth Des.* **2007**, *7*, 956.
(14) Welk, M. E.; Norquist, A. J.; Stern, C. L.; Poeppelmeier, K. R. *Inorg. Chem.* **2000**, *39*, 3946.
(15) Mahenthirarajah, T.; Lightfoot, P. *Chem. Commun.* **2008**, 1401.
(16) Pausewang, G. *Z. Anorg. Allg. Chem.* **1971**, *38*, 189.
(17) Waltersson, K. *Cryst. Struct. Commun.* **1978**, *7*, 507.

**Table 1.** Crystallographic Data

| | 1 | 2 | 3 | 4 | 5 | 6 |
|---|---|---|---|---|---|---|
| molecular formula | $[C_2H_8N][Cu(C_5H_5N)_4][V_2O_2F_7]$ | $[C_2H_8N][Cu(C_5H_5N)_4][V_2O_2F_7]$ | $[Cu(C_6H_7N)_4][VF_6]$ | $[C_3H_5N_2]_2[Cu(C_3H_4N_2)_4][V_2O_2F_8]$ | $[Cu_2F_2(C_{10}H_{10}N_3)_2][V_2O_7]$ | $[Cu(C_5H_5N)_2(C_2H_8N_2)][(VO_3)_2]$ |
| cryst syst | orthorhombic | triclinic | tetragonal | monoclinic | triclinic | orthorhombic |
| space group | *Pbcn* | $P\bar{1}$ | *P4/mcc* | $P2_1/n$ | $P\bar{1}$ | $P2_1\ 2_1\ 2_1$ |
| *a* (Å) | 15.291(4) | 8.981(3) | 8.988(2) | 11.024(2) | 8.047(2) | 10.972(3) |
| *b* (Å) | 9.806(3) | 13.533(6) | | 10.095(2) | 8.836(2) | 11.466(3) |
| *c* (Å) | 18.028(5) | 13.545(6) | 17.355(4) | 12.635(3) | 9.399(1) | 13.842(4) |
| α (deg) | | 89.15(3) | | | 65.53(2) | |
| *β* (deg) | | 70.64(2) | | 103.16(1) | 73.97(3) | |
| *γ* (deg) | | 74.19(3) | | | 78.14(3) | |
| *V* (Å$^3$) | 2703.0(1) | 1489.2(10) | 1402.0(5) | 1369.2(1) | 581.5(2) | 1741.4(8) |
| *Z* | 4 | 2 | 8 | 4 | 1 | 4 |
| total/unique reflns | 16186/2467 | 10224/5927 | 7904/671 | 9229/2809 | 4029/2209 | 11816/3614 |
| ind. reflns > 2$\sigma(I)$ | 1975 | 4651 | 617 | 2547 | 1671 | 2835 |
| fw | 692.91 | 692.91 | 593.16 | 759.94 | 723.40 | 477.72 |
| *T* (°C) | −180 | −180 | −180 | −180 | −180 | −180 |
| *λ* (Å) | 0.7107 | 0.7107 | 0.7107 | 0.7107 | 0.7107 | 0.7107 |
| $\rho_{calcd}$ (g/cm$^3$) | 1.70 | 1.55 | 1.42 | 1.84 | 2.07 | 1.82 |
| R1 [$I > 2\sigma(I)$] | 0.074 | 0.124 | 0.079 | 0.046 | 0.073 | 0.066 |
| wR2 [$I > 2\sigma(I)$] | 0.161 | 0.339 | 0.243 | 0.135 | 0.210 | 0.142 |

with the nearest terminal fluorine atoms of the $[V_2O_2F_7]^{3-}$ anion (N3−H3a/b···F, 1.90 Å; N3···F1, 2.79 Å).

Compound **2** is perhaps best regarded as a polymorph of **1**, although there is evidence from the X-ray refinement of the presence of some disordered solvent or guest moieties, which is supported by the observation that **2** is less stable in the air than **1**. The calculated density based on the given formula is, in fact, considerably lower than that of **1** (Table 1), and indeed, the unit cell packing (Figure 3) reveals a more "open" structure. The same basic chain motif is present in both **1** and **2**. The major differences lie in the interchain interactions, mediated by H bonding through the $[C_2H_8N]^+$ countercation, which in turn dictates the overall packing. In **1**, the dimethylammonium cation is positioned on a 2-fold axis and forms two symmetrically equivalent H bonds to one particular $[V_2O_2F_7]^{3-}$ anion of a single chain; there are no H-bonded interchain interactions. In **2**, on the other hand, the dimethylammonium cation forms hydrogen bonds (N5−H5b···F1, 2.07 Å; N5···F1, 2.84 Å; N5−H5a···F6, 1.91 Å; N5···F6, 2.74 Å) with two separate $[V_2O_2F_7]^{3-}$ anions of different chains (Figure 4). This difference makes a significant contribution both to the individual chain configurations and to the orientation of chains relative to each other. The relative chain configurations may be understood by comparing the Cu−V−V−Cu torsion angles, namely, 128.2° for **1** and 143.6° for **2**. The orientations of the chains may be understood by comparing key interchain distances: in **1**, the closest interchain V−V distances are about 7.2 Å, whereas in **2**, these alternate between 7.4 and 12.0 Å (Figures 2 and 3).

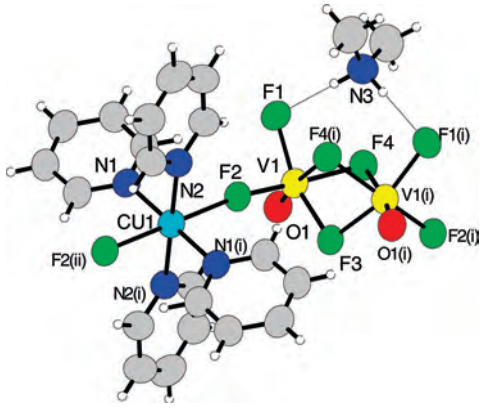


**Figure 1.** Building unit for **1** (50% probability ellipsoids). Symmetry operators (i) 2 − *x*, *y*, −3/2 − *z*; (ii) 2 − *x*, −*y*, −1 − *z*.

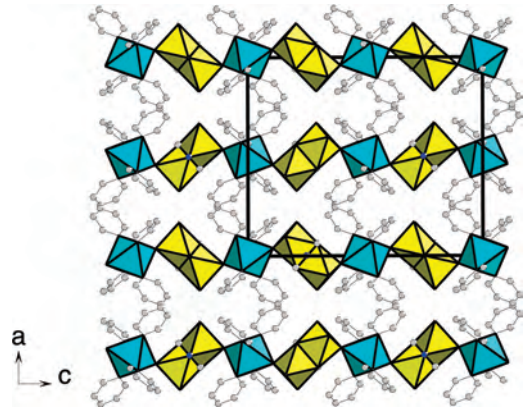


**Figure 2.** Unit cell packing for **1**. Hydrogen atoms not shown, for clarity.

The crystal structure of **3** exhibits a 1-D linear chain running along the *c* axis with the stoichiometry $[Cu(C_6H_7N)_4][VF_6]$, the anion $[VF_6]^{2-}$ and cation $[Cu(C_6H_7N)_4]^{2+}$ bound in an alternating manner by Cu−F−V linkages (Figure 5). The high symmetry of the crystal structure necessitates some disorder in the model, first due to the mirror plane running through the 3-methylpyridine ligand, which occupies the equatorial coordination sites on copper, and, second, due to the degree of freedom allowed at the equatorial F sites of the $[VF_6]$ octahedral unit, whereby the F atoms have been positioned as 4-fold disordered: there is no additional coordination to impose a preferred in-plane orientation. Bond valence sum analysis[18] reveals the V center to be $V^{4+}$; although uncommon in comparison to the $[VOF_5]^{3-}$ and the $[VF_6]^{3-}$ units, $[VF_6]^{2-}$ has been observed previously.[15,19] There is no hydrogen bonding or other interchain interaction in this structure.

(18) Brese, N. E.; O'Keeffe, M. *Acta Crystallogr.* **1991**, *B47*, 192.
(19) Becker, S.; Muller, B. G. *Angew. Chem., Int. Ed. Engl.* **1990**, *29*, 406.

**Table 2.** Selected Bond Lengths(Å), Angles (deg), and Bond Valence Sums[18] (∑, v.u.)[a]

| 1 | 2 | 3 | 4 | 5 | 6 |
|---|---|---|---|---|---|
| V1−O1 1.602(4) | V1−O1 1.598(7) | V1−F1 × 2 1.907(6) | V1−O1 1.605(2) | V1−O1 1.738(5) | V1−O1 1.638(5) |
| V1−F1 1.893(3) | V1−F1 1.895(5) | V1−F2 × 4 1.83(2) | V1−F1 1.918 (2) | V1−O2 1.770(1) | V1−O2 1.655(5) |
| V1−F2 1.904(3) | V1−F2 1.915(5) | Cu1−F1 × 2 2.432(1) | V1−F2 1.937(2) | V1−O3 1.653(5) | V1−O3 1.813(5) |
| V1−F3 1.997(3) | V1−F3 2.008(5) | Cu1−N1 × 4 2.033(5) | V1−F3 1.940(2) | V1−O4 1.693(5) | V1−O4 1.805(5) |
| V1−F4 1.945(3) | V1−F4 1.952(5) | Cu1−F1−V1 180.0(1) | V1−F4 2.202(2) | V1−O2−V1 180.0(1) | V2−O3 1.801(5) |
| V1−F4(i) 2.277(3) | V1−F5 2.317(5) | ∑(V1) 3.98 | V1−F4(ii) 1.964(2) | V1−O4−Cu1 124.0(1) | V2−O4 1.813(5) |
| V1−F4−V1(i) 89.0(1) | V2−O2 1.599(7) | ∑(Cu1) 1.99 | V1−F4−V1 106.5(1) | V1−O3−Cu1 118.6(1) | V2−O5 1.668(5) |
| V1−F3−V1(i) 96.1(1) | V2−F3 2.026(5) | | V1−O1−Cu1 161.1(1) | Cu1−F1−Cu1 101.7(1) | V2−O6 1.644(5) |
| F4−V1−F4(i) 73.1(1) | V2−F4 2.288(6) | | Cu1−O1 × 2.450(1) | Cu−F1 1.937(4) | V1−O3−V2 131.4(1) |
| F3−V1(i)−F4 71.4(1) | V2−F5 1.947(5) | | Cu1−N1 × 2 2.031(3) | Cu−F1(iii) 1.942(4) | V1−O4−V2 128.5(1) |
| F3−V1(i)−F4(i) 78.9(1) | V2−F6 1.909(5) | | Cu1−N2 × 2 2.017(3) | Cu−N1 1.974 (5) | V2−O5−Cu1 143.7(1) |
| F3−V1−F4(i) 71.4(1) | V2−F7 1.923(6) | | ∑(V1) 3.97 | Cu−N2 1.977 (5) | Cu1−O5 2.249(5) |
| F3−V1−F4 78.9(1) | V1−F3−V2 96.0 (1) | | ∑(Cu1) 2.13 | Cu−O3 2.485(1) | Cu1−N1 2.005(5) |
| V1−F3−V1(i) 96.1(1) | V1−F4−V2 89.6(1) | | | Cu−O4 2.466(1) | Cu1−N2 2.029(5) |
| V1−F4−V1(i) 89.0(1) | V1−F5−V2 88.9(1) | | | ∑(V1) 5.13 | Cu1−N3 2.055(6) |
| Cu1−F2−V1 171.6(1) | V1−F2−Cu1 174.3(1) | | | ∑(Cu1) 2.09 | Cu1−N4 2.036(6) |
| Cu1−F2 × 2 2.257(3) | V2−F7−Cu2 178.6(1) | | | | ∑(V1) 5.01 |
| Cu1−N1 × 2 2.063(5) | Cu1−F2 × 2 2.297(5) | | | | ∑(V2) 4.97 |
| Cu1−N2 × 2 2.045(5) | Cu1−N1 × 2 2.054(7) | | | | ∑(Cu1) 2.08 |
| ∑(V1) 3.98 | Cu1−N2 × 2 2.054(7) | | | | |
| ∑(Cu1) 2.09 | Cu2−F7 × 2 2.325(5) | | | | |
| | Cu2−N4 × 2 2.047(8) | | | | |
| | Cu2−N3 × 2 2.033(9) | | | | |
| | ∑(V1) 3.93 | | | | |
| | ∑(V2) 3.90 | | | | |
| | ∑(Cu1) 2.11 | | | | |
| | ∑(Cu2) 1.86 | | | | |

[a] Symmetry operators: (i) 2 − *x*, *y*, −3/2 − *z*; (ii) 1 − *x*, −*y*, −*z*; (iii) 1 − *x*, −*y*, 1 − *z*.

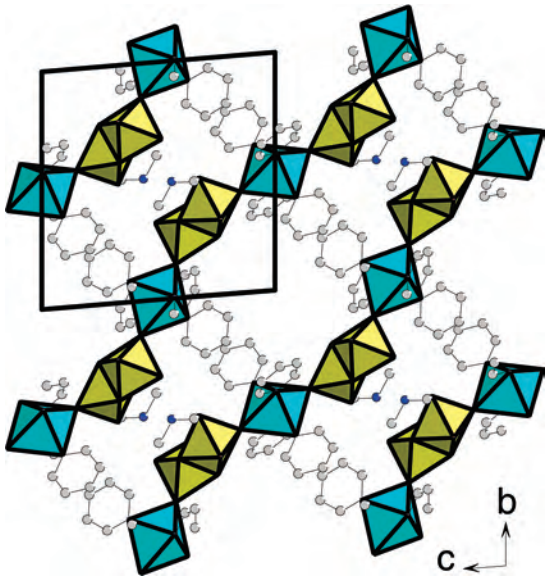


**Figure 3.** Unit cell packing for **2**. Hydrogen atoms not shown.

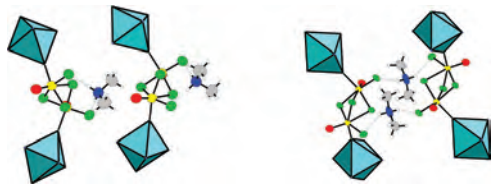

**Figure 4.** Hydrogen-bonding interactions mediated by the dimethylamine cations: (a) *intra*-chain only in **1**; (b) *inter*-chain H-bonding in **2**.

The structure of **4** reveals an infinite 1-D chain propagating along the *a* axis, with the formula $[Cu(C_3H_4N_2)_4][V_2O_2F_8]$. The imidazole acts as both a protonated template and a neutral ligand to $Cu^{2+}$ in this case. Vanadium once again adopts the +4 oxidation state, and occurs in an edge-sharing dimeric unit $[V_2O_2F_8]^{4-}$, which we have previously seen in both organically templated VOFs[9] and in the inorganic compound $Na_4V_2O_2F_8$.[20] The building unit is shown in Figure 6, and the crystal packing is shown in Figure 7. The crystal packing is stabilized by hydrogen-bond interactions between the imidazolium cations and the F atoms of the chain, and also *via* direct H bonds from the $[Cu(C_3H_4N_2)_4]^{2+}$ moiety to neighboring chains, leading to a 3-D supramolecular network. The protonated imidazole moieties form relatively strong hydrogen bonds with contacts in the ranges N−H···F = 1.73−1.85 Å and N···F = 2.57−2.69 Å. The direct interchain interactions from the $[Cu(C_3H_4N_2)_4]^{2+}$ cation are somewhat weaker: N−H···F and N···F distances in the range of 2.05−2.19 Å and 2.76−2.82 Å, respectively. The overall result is that all of the F atoms are involved as H-bond acceptors.

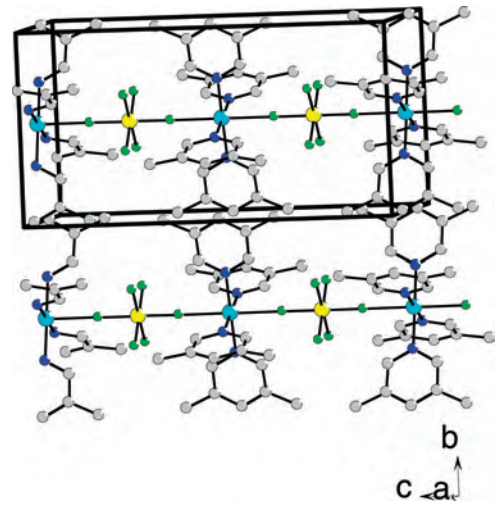


**Figure 5.** Unit cell packing of **3** (H atoms and disordered F atoms not shown).

(20) Aldous, D. W.; Lightfoot, P. Submitted for publication.

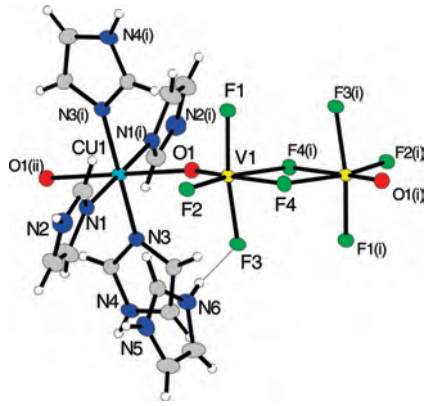


**Figure 6.** Building unit for **4** (50% probability ellipsoids). Symmetry operators (i) $1 - x, -y, -z$; (ii) $2 - x, -y, -z$.

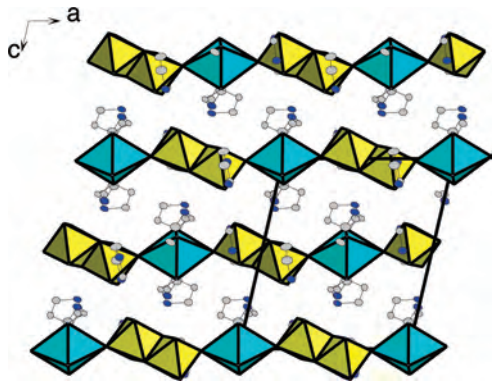


**Figure 7.** Crystal packing for **4**. Hydrogen atoms not shown.

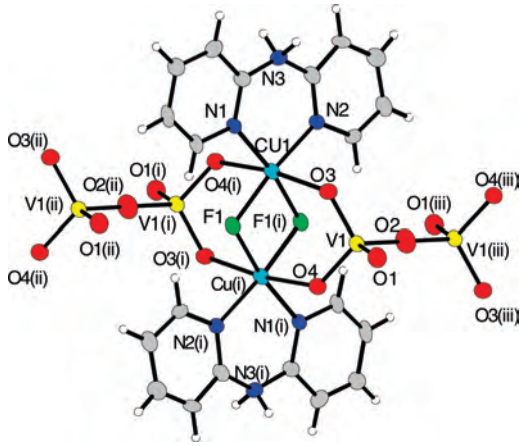


**Figure 8.** Dimeric building unit in **5** (50% probability ellipsoids). Symmetry operators (i) $1 - x, -y, 1 - z$; (ii) $-1 + x, y, z$; (iii) $2 - x, -y, 1 - z$.

Compound **5** crystallizes as a hybrid inorganic/organic 1-D infinite chain extending along the *a* axis. The building unit consists of a dimeric $[Cu_2F_2(C_{10}H_{10}N_3)_2]^{4+}$ complex situated on an inversion center and linked *via* $[V_2O_7]^{4-}$ anionic units through oxygen ligands. Unusually in this series, the fluoride is therefore contained exclusively within the coordination sphere of copper rather than vanadium, acting as a bridge between the two edge-sharing Cu-centered octahedra (Figure 8). The axial sites of the cation motif connect to the $[V_2O_7]^{4-}$ anions, which unusually have a 180° V−O−V bond angle, and the outer equatorial sites are occupied by a bidentate dipyridylamine ligand. The vanadium oxidation state is confirmed as +5 by BVS analysis (Table 2). A similar

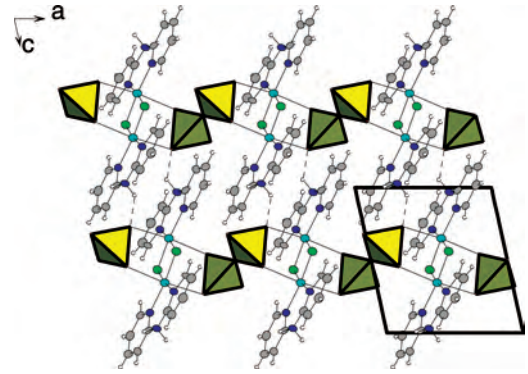


**Figure 9.** Crystal packing in **5**.

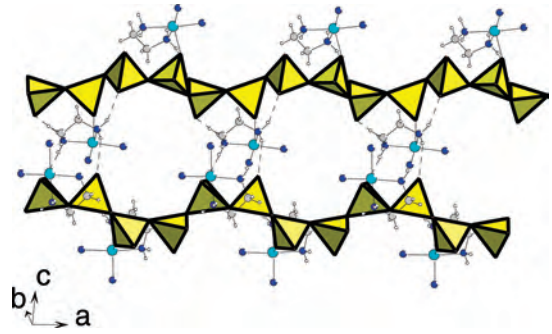


**Figure 10.** Infinite $[VO_2O_{2/2}]^-$ tetrahedral chains decorated by Cu complexes in **6**.

cationic moiety, bridged by $[SiF_6]^{2-}$ rather than $[V_2O_7]^{4-}$, has been reported previously,[21] but in the present case, the dipyridylamine is protonated due to the strongly acidic conditions in the HF reaction medium. Crystal packing is dominated by hydrogen bonds from the protonated dipyridylamine to the anion of a neighboring chain (Figure 9), leading to supramolecular 3-D network interactions (N3−H3b···O3, 2.24Å; N3···O3, 2.86 Å).

The crystal structure of **6** is exceptional in this context, as it is the only case in which fluoride is not incorporated into the product. Instead, infinite corner-sharing chains of vanadate tetrahedra occur, $[VO_2O_{2/2}]^-$, which is a common structural motif in hybrid copper−vanadium oxide chemistry, for example, in $Cu(bipy)_2[V_2O_6]$.[2,22] The $[VO_2O_{2/2}]^-$ motif consists of four tetrahedra per chain repeating units propagating along the *a* axis. There are two crystallographically independent vanadate tetrahedra, which alternate along the chain, only one of which coordinates to the Cu-containing moiety. The Cu center itself is unusual in containing two different, coordinating N-donor ligands, *py* and *en*, leading to overall square-pyramidal coordination around Cu (Figure 10). Effectively, the copper complex in this case acts as "decoration" to the vanadium oxide chain, rather than being directly involved in chain formation itself. There are weak intrachain and interchain hydrogen-bonding interactions (N1···O1, 2.97 Å; N2···O6, 2.86 Å, respectively) between the ethylenediammonium moiety and the $[VO_2O_{2/2}]$ unit, which is not bonded to the cation directly, in the case of the intrachain interaction.

(21) Casellas, H.; Pevec, A.; Kozlevcar, B.; Gamez, P.; Reedijk, J. *Polyhedron* **2005**, *24*, 1549.
(22) Debord, J. R. D.; Zhang, Y.; Haushalter, R. C.; Zubieta, J.; O'Connor, C. J. *J. Solid State Chem.* **1996**, *122*, 251.

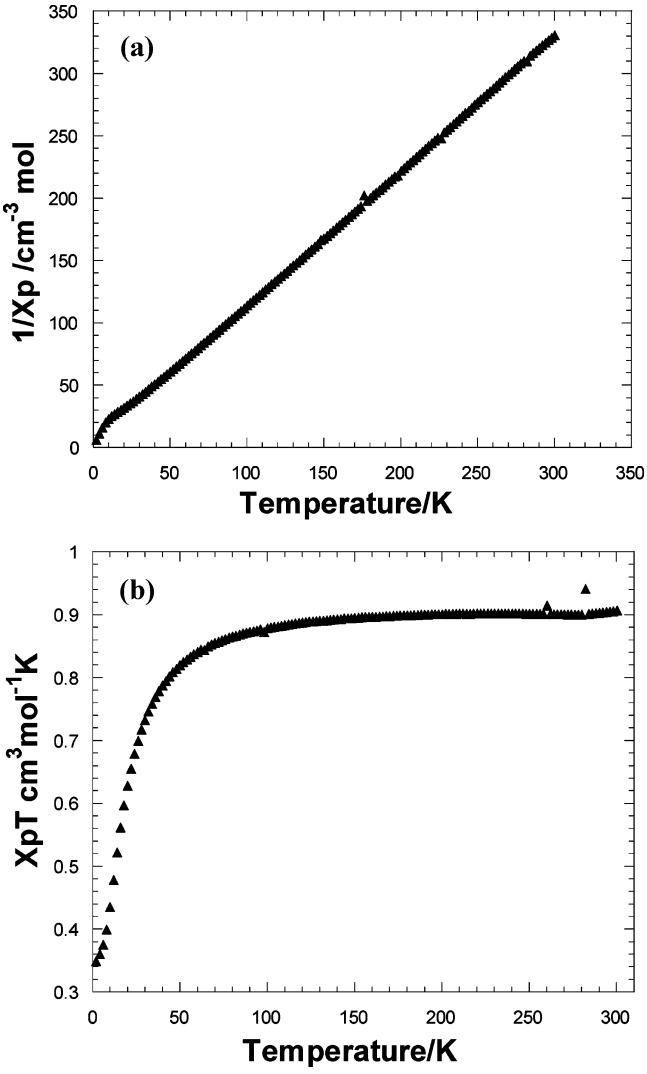


**Figure 11.** (a) $1/\chi_p$ versus T and (b) $\chi_pT$ versus T for **1**.

**Magnetic Suceptibilities.** Due to problems with sample stability and purity, magnetic data were collected for only samples **1** and **3**.

Above 50 K, the magnetic susceptibility for **1** obeys a Curie−Weiss law (Figure 11a), with no evidence of long-range magnetic ordering. A fit to the $1/\chi_p$ versus $T$ plot reveals a negative Weiss constant ($\theta = -5.0$ K), and the falloff of $\chi_pT$ versus $T$ reveals short-range antiferromagnetic correlations between the metal centers (Figure 11b). This is consistent with the study of Darriet et al.[23] on $Cs_3V_2O_2F_7$. The value of $C = 0.922$ cm$^3$ mol$^{-1}$ K ($\mu_{eff} = 2.72\ \mu_B$), obtained from the Curie−Weiss plot, is consistent with the ideal system of three noninteracting isolated spin −1/2 centers per formula unit ($\mu_{ideal} = 3\ \mu_B$), also confirming the BVS analysis of $V^{4+}$ and $Cu^{2+}$. Below 50 K, deviations from the Curie−Weiss behavior may be expected due to the alternating V−V and V−Cu interactions along the chain (V−V separation within the face-sharing dimer is 2.97 Å, whereas the V−Cu distance is 4.15 Å).

The magnetic susceptibility data for **3** fit very well to a Curie−Weiss law in the range of 50−300 K. The linear plot of $1/\chi_p$ versus $T$ (Figure 12) reveals paramagnetism, with a small positive Weiss constant ($\theta = +1.66$ K), suggesting a tendency toward weak ferromagnetic interactions. The value of $C = 0.585$ cm$^3$ mol$^{-1}$ K ($\mu_{eff} = 2.16\ \mu_B$) is slightly lower than the theoretical value of $\mu_{ideal} = 2.45\ \mu_B$ for two noninteracting spin −1/2 centers.

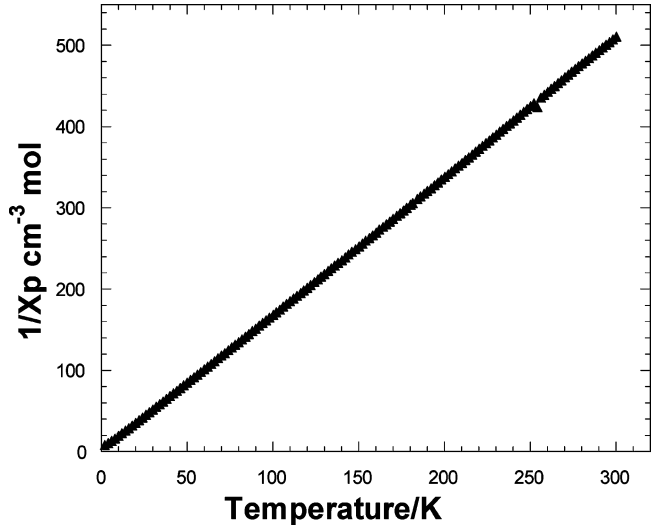


**Figure 12.** $1/\chi_p$ versus T for **3**.

## Concluding Remarks

Our preliminary exploration toward the hydrothermal chemistry of vanadium oxyfluorides incorporating copper coordination complexes has produced the six novel chainlike structures reported here. These expand on the previous mixed V/Cu oxyfluoride hybrids reported by ourselves[15] and by Poeppelmeier[13,14] and also complement the plethora of VOF oligomeric and chain structures we have noted in previous work. Novel structural features are present in each case, either in the incorporation of dimeric VOF units into chains, as in **1**, **2**, and **4**; or in the presence of amines acting as both the ligand and template (**4**); or in the presence of unusual mixed ligand copper complexes (**5** and **6**). As anticipated in such complex systems, it is currently impossible to predict the outcome of each reaction, with subtle parameter changes leading to subtle variations on a theme (e.g., **1** and **2**) often dictated by H bonding or other supramolecular effects. The key factors which govern the nature of the VOF units produced in these reactions, and also their mode of linkage into chain fragments or other extended moieties, can only be determined with a considerable amount of further experimentation.

**Acknowledgment.** We thank Prof. Alex Slawin for assistance in collecting the diffraction data, Dr. Richard Goff and Dr. David Aldous for help with the magnetic measurements, and EaStCHEM for a Prize Studentship to T.M.

**Supporting Information Available:** Crystallographic data in CIF format. This material is available free of charge via the Internet at http://pubs.acs.org.

IC801106H

(23) Darriet, J.; Bonjour, E.; Beltran-Porter, D.; Drillon, D. *J. Magn. Magn. Mater.* **1984**, *44*, 287.